CIÊNCIA EXATAS E DA TERRA

Scientia Amazonia, v. 11, n.3, C16-C31, 2022
Revista on-line http://www.scientia-amazonia.org
https://doi.org/10.5281/zenodo.7510994 - ISSN:2238.1910

Caracterização do derivado ácido de Meldrum complexado com zinco por espectroscopias FT-IR, FT-Raman e cálculos DFT

Rodolfo Sebastião Estupiñán Allan[1], João Antunes da Silva[2], Thiago Andrade de Toledo[3], Tarun Yadav[4], Ricardo Rodrigues de França Bento[5]

Resumo

Neste estudo, relatamos a caracterização de um derivado do ácido de Meldrum complexado com Zinco, Bis[2,2-Dimetil-5-(2-piridil-aminometileno)-[1,3]dioxan-4,6-diona]Zinco (C24H24N4O10Zn), preparado pela reação direta entre a superfície e o ligante. As propriedades estruturais e espectroscópicas do composto acima foram investigadas usando espectroscopias de infravermelho com transformada de Fourier e Raman combinadas com teoria do funcional da densidade (DFT) com conjunto de base B3LYP/6-31G (d,p), para avaliar informações sobre as preferências conformacionais moleculares e atribuições vibracionais . As atribuições do modo vibracional são discutidas com base na análise da distribuição de energia potencial (PED). Uma análise comparativa dos parâmetros geométricos estruturais dos derivados de ácido de Meldrum não complexado e complexado foi feita, e uma completa análise dos modos vibracionais foi fornecida para o derivado ácido de Meldrum complexado com zinco.

Palavras-Chave: Espalhamento Raman; Espectroscopia IR; PED; Ácido de Meldrum; Complexos de zinco

Characterization of zinc complexed Meldrum's acid derivative by FT-IR and FT-Raman spectroscopies and DFT calculations. In this study, we report the characterization of a chosen Meldrum's acid derivative complexed with Zinc, Bis[2,2-Dimethyl-5-(2-pyridyl-aminomethylene)-[1,3]dioxan-4,6-dione]Zinc ($C_{24}H_{24}N_4O_{10}Zn$), prepared by the direct reaction between the binder and ligand. The structural and spectroscopic properties of above compound were investigated using Fourier Transform Infrared and Raman spectroscopies combined with functional theory (DFT) with B3LYP/6-31G (d,p) basis set, to evaluate information on the molecular conformational preferences and vibrational assignments. The vibrational mode assignments are discussed based on potential energy distribution (PED) analysis. A comparative analysis of the structural geometric parameters of the uncomplexed and complexed Meldrum acid derivatives was carried out, and a complete analysis of the vibrational modes was provided for the zinc complexed Meldrum acid derivative.

Keywords: Raman scattering; IR spectroscopy; PED; Meldrum's Acid; Zn complexes.

[1] Professor Assistente, Departamento de Matemática, UFMT, rodolfo.allan@gmail.com
[2] Professor Titular, Secretaria de Estado de Educação, SEDUC-MT, jas.antuness@gmail.com
[3] Professor Adjunto, UFMT, toledo@fisica.ufmt.br
[4] Associate Professor, Institute of Science, Department of Physics, Banaras Hindu University, Varanasi, India tarunyadavbly@gmail.com
[5] Professor Associado, Instituto de Física, UFMT, ricardobento@fisica.ufmt.br

Scientia Amazonia, v. 11, n.3, C16-C31, 2022
Revista on-line http://www.scientia-amazonia.org
https://doi.org/10.5281/zenodo.7510994 - ISSN:2238.1910

1. Introduction

Meldrum's acid and its derivatives have been used in syntheses of heterocyclics. It was synthesized in 1908 by the reaction between acetone and malonic acid in the presence of acetic anhydride and sulfuric acid, being very important and popular reagent in organic synthesis, mainly in the synthesis and design of organic compounds used in the context of drugs and pharmaceuticals (CALISKAN 2017; GHOSH 2011; SHAHCHERAGH 2017; IVANOV 2008; JANIKOWSKA 2014; LIPSON 2009; SAMPAIO 2013). Pyridines and pyrimidines are among the simplest heterocycles and play an important role in basic vital functions in the life of living beings. Its main structure is found in nucleotides and in several alkaloids (SEVENARD 2017; LINDEMAN 1993; MELDRUM 1908). In the last decades, there was an increase in interest by identify their chemical components using nondestructive techniques (MCNAB 1987; CHEN 1991; URLAUB 1997; SCHRADER 1999; MICIC 2003; FEHR 2004; RADOTIC 2005).

Yavari applied it to organic systems, synthetizing several compounds with Meldrum's acid (YAVARI 2005) while Chaudary et al investigated its applications in the field of green chemistry, describing the multicomponent reaction involving Meldrum's Acid (CHAUDHARY 2016). The derivatives of Meldrum's acid are usually related to several proven biological properties and have antibacterial potential (SILVA 2007; SAMPAIO 2014; MOHSSEN 2017). The applications and properties of some Meldrum's acid derivatives were greatly discussed (JANIKOWSKA 2014). The molecule C24H24N4O10Zn of family heterocyclics, is a compound with great medicinal importance and a wide range of biological activities, are also known as useful oxidation inhibitors, cyanine dyes, metal chelating agents and anti-corrosion agents (DACI-AJVAZI 2011). The use of platinum-based drugs in the cancer chemotherapy promoted as increase of developing inorganic pharmaceutical agents in medicinal chemistry using biological trace metals such as Zn. These complexes are antioxidants useful in reduction the side effects caused by chemotherapy and radiotherapy.

There is solid evidence that antioxidants, by helping to reduce the tumor and prolong the life expectancy of patients, may be a good choice for therapeutic intervention with chemotherapy (TOLEDO 2012). Therefore, metal complexes based on structures may be useful alternatives to treat incurable diseases (YOSHIKAWA 2012; ABRAHAM 2008; SUBRAMANIAN 2010; SINHA 2004; KOHN 1996). In this work, we report the characterization of the Meldrum's acid derivative C24H24N4O10Zn, performed by FT-IR and FT-Raman techniques and DFT calculations. The FT-IR and FT-Raman spectra of the molecule were recorded at room temperature and was used B3LYP/6-31G(d,p) method to assignment the normal modes of the molecule. Moreover, we used VEDA (JAMRÓZ 2001) software to analyze of the potential energy distribution (PED).

2. Material e Method

2.1 Synthesis process

The zinc complex was prepared by the direct reaction between the binder and zinc chloride. The addition of base (NH4OH) for deprotonation of amidic nitrogen obtained the zinc complexes (YOSHIKAWA 2012; ABRAHAM 2008; SUBRAMANIAN 2010; SINHA 2004) The procedure can be summarized as follows: 2 mmol of the binder was dissolved in 30 ml of methanol and 3 drops of NH4OH base were added. This solution was magnetically stirred and 1 mmol of ZnCl2 was dissolved in hot methanol and dripped in methanolic solution of the binder.

Scientia Amazonia, v. 11, n.3, C16-C31, 2022
Revista on-line http://www.scientia-amazonia.org
https://doi.org/10.5281/zenodo.7510994 - ISSN:2238.1910

2.2 Spectroscopic characterization

The FT-IR spectrum was obtained using a Shimadzu Prestige-21 Spectrometer with range within 3700-400 cm^{-1}, with spectral resolution of 4 cm^{-1} and the spectra accumulated over 20 scans. The samples were prepared in KBr disc. The FT-Raman spectrum was obtained using a Bruker Optics, Vertex 70, Ram module II laser Nd: YAG at 1064 nm line with a power of 60 mW. The spectra were recorded in the spectral region 50 to 3250 cm^{-1}.

2.3 Computational Methods

The density functional theory (DFT) calculations were done with Becke's 3-parameter hybrid combined with the Lee-Young–Parr correlation functional (B3LYP) (LEE 1988; BECKE 1988). No restriction of symmetry was imposed on the initial structure. The molecule, $C_{24}H_{24}N_4O_{10}Zn$, was optimized structural parameters and vibrational wavenumbers were performed with restricted B3LYP with 6-31G (d,p) basis set. The calculations were done using Gaussian 09 software with a single molecule of each, in gas phase. There was no imaginary frequency on the calculated optimized structure (ABRAHAM 2008; DHAOUADI 2009). The harmonic vibrational frequencies were calculated at the optimized geometries using the same theoretical method. Also, the harmonic force constant was obtained using DFT calculations, to predict the fundamental vibrational wavenumber for comparison with experimental results. We have used a pure Lorentzian band shape with a bandwidth (FWHM) of 10 cm^{-1} to plot the simulated spectra.

3. Results and Discussion

3.1 Molecular Structure

The Meldrum's acid derivative complexed with zinc is made from two copies of $C_{12}H_{12}N_4O_5$ united by the Zinc. In the Figure 1 we can see the proposed molecular structure, $C_{24}H_{24}N_4O_{10}Zn$.

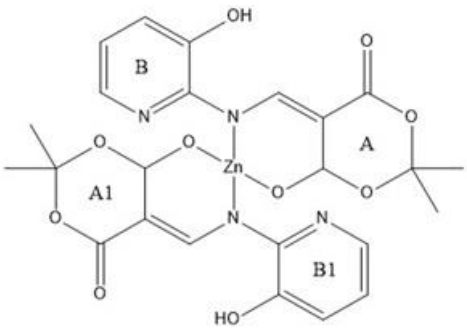

Figure 1: The molecular structure of $C_{24}H_{24}N_4O_{10}Zn$. The molecule is symmetric and have two Meldrum's rings and two Pyridine rings.

The rings **A** and **A1** are referent to Meldrum's acid rings and **B** and **B1** referent to Pyridine rings. It is relevant to remember that pyridine has a conjugated system of six π electrons that are delocalized over the ring and therefore, a weaker resonant stabilization than benzene (JOULE 2010). Rings **A** and **B** (as well as **A1** and **B1**) are connected by an amino chain where the zinc complexation took place. We can see at Figure 2 the atoms

Scientia Amazonia, v. 11, n.3, C16-C31, 2022
Revista on-line http://www.scientia-amazonia.org
https://doi.org/10.5281/zenodo.7510994 - ISSN:2238.1910

naming map that we adopted for purposes of this study. We have named by atom type and number in group.

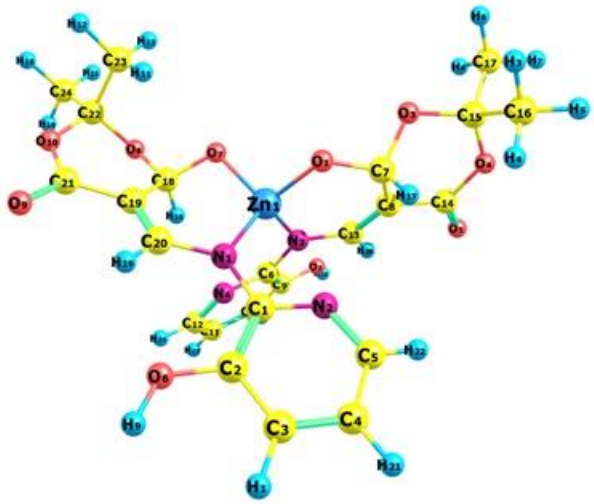

Figure 2: The molecular structure and numbering label of $C_{24}H_{24}N_4O_{10}Zn$. The atoms were labeled by type and number in group. The rings components are A – C18-C19-C21-O10-C22-O8, A1 – C7-C8-C14-O4-C15-O3, B – C1-C2-C3-C4-C5-N2 and B1 – C6-C9-C10-C11-C12-N4.

Using Table 1, we have compared our molecule geometry with a non-complexed Meldrum's acid derivative, 2,2-Dimethyl-5-(2-pyridyl-aminomethylene)-[1,3]dioxan-4,6-dione ($C_{12}H_{12}N_2O_4$) (NCBI 2022), to establish some conclusions about the complexation process (SHI 2011). We have chosen this derivative for its strong similarities with both our molecules. The major conclusion which was drawn is that there are large disturbances around near the metal, the bonds and angles became larger to adapt the new structure after the complexation process.

Table 1: Comparison of geometric experimental parameters between C12H12N2O4 and C24H24N4O10Zn, where we can see the expected molecular displacement.

Bond	**Lengths (Å)**	
	$C_{12}H_{12}N_2O_4$	$C_{24}H_{24}N_4O_{10}Zn$
O1-H4	0,9611	0,9680
C3-H1	1,0821	1,0829
C4-H2	1,0818	1,0320
C5-H3	1,0801	1,0320
C8-H5	1,0901	1,0797
C11-H7	1,1088	1,1091
C11-H8	1,1163	1,1111
C11-H9	1,1099	1,1112
C12-H10	1,1083	1,1112
C12-H11	1,1108	1,1116
C12-H12	1,1145	1,1114
O4-C9	1,2207	1,3935

Scientia Amazonia, v. 11, n.3, C16-C31, 2022
Revista on-line http://www.scientia-amazonia.org
https://doi.org/10.5281/zenodo.7510994 - ISSN:2238.1910

Bond	Lengths (Å)	
	$C_{12}H_{12}N_2O_4$	$C_{24}H_{24}N_4O_{10}Zn$
C7-C8	1,3160	1,3545
C4-C3	1,3928	1,3930
C5-C4	1,3929	1,3912
C2-C3	1,3985	1,4039
N2-C1	1,3565	1,3614
N2-C5	1,3605	1,3571
O1-C2	1,3306	1,3472
N1-C8	1,3764	1,4253
O5-C9	1,3427	1,4264
N1-C1	1,4241	1,4271
C9-C7	1,4775	1,5286
O5-C10	1,3822	1,4219
C11-C10	1,5345	1,5453
O3-C6	1,4472	1,3475
O3-C10	1,4454	1,3839
O2-C6	1,4546	1,2216
C12-C10	1,5562	1,5310
Bond	**Angles (°)**	
	C12H12N2O4	**C24H24N4O10Zn**
C7-C12-N2	125,03	122,03
C2-C3-C4	119,64	120,45
H10-C3-C4	120,64	119,80
H9-C5-N1	115,69	119,91
H8-C12-N2	118,14	108,36
H6-C11-H5	109,08	108,76
H4-C11-H6	109,12	108,36
H5-C11-H4	109,34	108,34
H2-C10-H1	108,56	108,83
H1-C10-H3	108,49	109,74
H3-C10-H2	109,21	119,16
O1-C6-O2	118,90	123,06
C3-C4-C5	117,81	119,93
C1-N1-C5	117,79	119,16
N1-C5-C4	123,64	127,26
C12-N2-C1	127,87	116,91
O2-C6-C7	116,37	123,61
N2-C1-N1	113,11	114,77
C6-C7-C12	121,37	107,66
C9-O2-C6	118,98	121,34
C11-C9-O2	105,87	110,52
C8-O4-C9	119,44	119,77
O4-C9-O2	111,89	111,65

CIÊNCIA EXATAS E DA TERRA

Scientia Amazonia, v. 11, n.3, C16-C31, 2022
Revista on-line http://www.scientia-amazonia.org
https://doi.org/10.5281/zenodo.7510994 - ISSN:2238.1910

3.2 Vibrational Analysis

The $C_{24}H_{24}N_4O_{10}Zn$ has 183 normal vibrational modes, excluding the three rotational and three translational modes. We can see at Figure 3 the molecular structure and numbering label of $C_{12}H_{12}N_2O_4$.

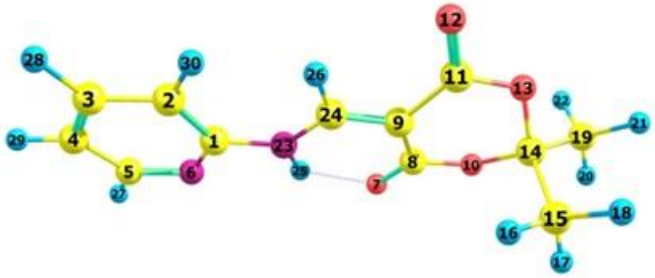

Figure 3: The molecular structure and numbering label of $C_{12}H_{12}N_2O_4$. The atoms were labeled by type and number in group.

We have used VEDA software to assign those modes. The theoretical spectra were adjusted with the experimental one using a scale factor of 0.9613. This scale is used to minimize overestimation factor, for instance, an incomplete basis set or vibrational anharmonicity (SINHA 2004), and usually this factor is a semi empirical number between 0.96 and 0.99 (CORREDOR 2009). Through PED basis analysis, we have performed vibrational assignment of the normal modes of the molecules. PED values below 10% were disregarded for purposes of this study. Table 2 provides the calculated wavenumbers (in cm^{-1}), scaled factors, measured FT-Raman and FT-IR band position (in cm^{-1}) and assignments with PED. In this Table is listed the experimental and theoretical wavenumber along with their tentative assignments based on PED analysis.

Table 2: Calculated vibrational wavenumbers (in cm^{-1}) unscaled and scaled by the scale factor 0.9613, experimental IR and Raman band positions in units of cm^{-1} and assignment of vibrational modes for $C_{24}H_{24}N_4O_{10}Zn$.

#	ω_{calc}	ω_{scal}	ω_{FT_IR}	ω_{Raman}	Assignment with PED* (%)
1	61	59			δ (C6-N3-Zn1)(15)+τ (O4-C14-C8-C13)(14)
2	64	62			δ (Zn1-N1-C1)(26)+τ (C19-C20-N1-Zn1)(11)
3	74	71			τ (C22-O10-C21-C19)(17)
4	82	79			δ (C6-N3-Zn1)(15)+τ (O4-C14-C8-C13)(20)
5	102	98			τ (C22-O10-C21-C19)(14)+τ (O8-C22-O10-C21)(33)+τ (O10-C21-C19-C20)(16)
6	107	103		108m	δ (C20-N1-Zn1)(14)+δ (Zn1-N1-C1)(14)+δ (C13-N3-Zn1)(24)
7	119	114			γ (O6-C3-C1-C2)(10)+τ (Zn1-N1-C1-C2)(17)+τ (H9-O6-C2-C3)(13)
8	122	117			τ (N4-C6-N3-Zn1)(12)+τ (C12-N4-C6-N3)(18)
9	137	132		127w	δ (C21-C19-C20)(12)
10	140	135			τ (C10-C11-C12-N4)(14)

CIÊNCIA EXATAS E DA TERRA

Scientia Amazonia, v. 11, n.3, C16-C31, 2022
Revista on-line http://www.scientia-amazonia.org
https://doi.org/10.5281/zenodo.7510994 - ISSN:2238.1910

#	ωcalc	ωscal	ωFT_IR	ωRaman	Assignment with PED* (%)
11	154	148			γ (N1-C2-N2-C1)(21)+τ (H22-C5-N2-C1)(13)+τ (C2-C3-C4-C5)(10)+τ (H21-C4-C5-N2)(12)
12	156	150			τ (Zn1-N1-C1-C2)(13)
13	164	158			τ (C7-O3-C15-O4)(10)
14	167	160			τ (N4-C6-N3-Zn1)(13)+τ (H23-C11-C12-N4)(13)+τ (C12-N4-C6-N3)(11)+τ (H24-C12-N4-C6)(12)
15	180	173			δ (C20-N1-Zn1)(17)
16	182	175			γ (O6-C3-C1-C2)(14)+τ (H9-O6-C2-C3)(39)+τ (C3-C4-C5-N2)(13)
17	193	185			γ (O2-C10-C6-C9)(18)+τ (H18-O2-C9-C10)(51)
18	242	233			τ (C9-C10-C11-C12)(11)+τ (C11-C12-N4-C6)(10)+τ (H18-O2-C9-C10)(14)
19	257	247			ν (Zn1-N3)(14)
20	262	252			δ (C17-C15-O3)(23)
21	268	258			δ (C23-C22-O10)(14)+γ (C24-C23-O10-C22)(11)
22	335	322			δ (C24-C22-O10)(23)+δ (O10-C21-C19)(12)
23	349	335			γ (C17-C16-O3-C15)(38)+δ (O5-C14-O4)(12)
24	362	348			δ (C16-C15-O3)(54)
25	369	355			γ (C13-Zn1-C6-N3)(15)
26	373	358			δ (C23-C22-O10)(10)
27	391	376			δ (C23-C22-O10)(11)+δ (C24-C22-O10)(10)
28	410	394			δ (C16-C15-O3)(16)+δ (C17-C15-O3)(24)
29	415	399			τ (H3-C16-C15-C17)(16)+γ (C24-C23-O10-C22)(10)+τ (H4-C16-C15-C17)(14)+τ (H5-C16-C15-C17)(15)
30	418	402			δ (C23-C22-O10)(18)+γ (C24-C23-O10-C22)(19)
31	423	407			τ (H11-C23-C22-C24)(19)+τ (H13-C23-C22-C24)(10)+τ (H12-C23-C22-C24)(13)+τ (H16-C24-C22-C23)(17)+τ (H15-C24-C22-C23)(18)
32	443	426			τ (C9-C10-C11-C12)(10)
33	453	435			τ (H14-C24-C22-C23)(11)+τ (H11-C23-C22-C24)(11)
34	454	436			τ (H8-C17-C15-C16)(13)+τ (H6-C17-C15-C16)(16)+τ (H7-C17-C15-C16)(15)
35	458	440			δ (O6-C2-C3)(18)
36	465	447			δ (O6-C2-C3)(25)
37	467	449			ν (Zn1-N3)(11)+δ (O2-C9-C10)(28)
38	482	463			γ (C17-C16-O3-C15)(17)+δ (O3-C15-O4)(18)
39	494	475			γ (C23-O8-O10-C22)(12)+δ (C22-O10-C21)(15)+δ (O8-C22-O10)(12)+δ (C24-C22-O10)(12)
40	507	487			δ (O9-C21-O10)(10)
41	509	489			γ (C16-O4-O3-C15)(35)
42	513	493			τ (C1-N2-C5-C4)(16)+τ (H21-C4-C5-N2)(13)
43	515	495		499w	τ (H23-C11-C12-N4)(10)

Scientia Amazonia, v. 11, n.3, C16-C31, 2022
Revista on-line http://www.scientia-amazonia.org
https://doi.org/10.5281/zenodo.7510994 - ISSN:2238.1910

#	ωcalc	ωscal	ωFT_IR	ωRaman	Assignment with PED* (%)
44	532	511			γ (C23-O8-O10-C22)(14)
45	551	530			γ (O6-C3-C1-C2)(21)+γ (N1-C2-N2-C1)(17)
46	553	531			γ (O2-C10-C6-C9)(15)
47	562	540			δ (C2-C3-C4)(15)
48	567	545			δ (C11-C12-N4)(12)+δ (C9-C10-C11)(17)
49	585	562			δ (C15-O4-C14)(10)
50	593	570			δ (C22-O10-C21)(12)
51	620	596			δ (C9-C10-C11)(11)+δ (C10-C11-C12)(24)
52	628	604			δ (C2-C3-C4)(11)+δ (O9-C21-O10)(11)+δ (C3-C4-C5)(22)
53	647	622		623w	δ (O5-C14-O4)(12)
54	665	639	642w		γ (O5-C8-O4-C14)(21)
55	716	688	667m		ν (O8-C22)(12)+γ (O9-C19-O10-C21)(45)
56	721	693			δ (O7-C18-O8)(13)+δ (O10-C21-C19)(11)
57	724	696			τ (C11-C12-N4-C6)(21)+δ (O1-C7-O3)(13)+τ (H24-C12-N4-C6)(17)+ +ν (O3-C15)(12)
58	726	698			τ (C1-N2-C5-C4)(13)+τ (H22-C5-N2-C1)(21)+τ (C3-C4-C5-N2)(20)
59	748	719			γ (O5-C8-O4-C14)(24)+δ (O4-C14-C8)(10)
60	756	727			γ (O9-C19-O10-C21)(12)
61	760	730			γ (O6-C3-C1-C2)(16)+γ (N1-C2-N2-C1)(14)+τ (C1-N2-C5-C4)(10)
62	767	737			γ (O2-C10-C6-C9)(13)+τ (C9-C10-C11-C12)(10)+τ (C11-C12-N4-C6)(19)
63	790	759	757w		γ (O1-C8-O3-C7)(11)
64	797	766	771w		δ (O7-C18-O8)(21)+γ (O7-C19-O8-C18)(13)
65	819	787	782m		ν (O6-C2)(11)+δ (N2-C5-C4)(22)
66	838	805	811s		δ (C11-C12-N4)(15)
67	874	840			ν (O8-C22)(10)
68	879	845			ν (C16-C15)(13)+δ (O1-C7-O3)(15)
69	881	847			τ (H1-C3-C2-C1)(64)
70	882	848	854w		τ (H2-C10-C11-C12)(72)
71	901	866			τ (H19-C20-C19-C18)(22)+ν (N1-C1)(12)
72	914	878			δ (C12-N4-C6)(10)
73	936	899		891w	τ (H20-C13-C8-C7)(71)
74	943	906			ν (C23-C22)(18)+τ (H19-C20-C19-C18)(25)
75	951	914			ν (C23-C22)(14)+τ (H19-C20-C19-C18)(15)+ν (O8-C22)(11)
76	956	919	917vw		τ (H3-C16-C15-C17)(13)+ν (C16-C15)(10)+ν (C17-C15)(23)+ +τ (H5-C16-C15-C17)(10)
77	967	929	931w		ν (O3-C15)(15)
78	979	941			τ (H13-C23-C22-C24)(18)+τ (H12-C23-C22-C24)(11)+ν (C24-C22)(24)
79	1000	961	960w		δ (H21-C4-C5)(25)+ν (N2-C5)(15)+ν (N1-C20)(15)
80	1010	971			δ (H18-O2-C9)(10)+δ (H23-C11-C12)(33)

Scientia Amazonia, v. 11, n.3, C16-C31, 2022
Revista on-line http://www.scientia-amazonia.org
https://doi.org/10.5281/zenodo.7510994 - ISSN:2238.1910

#	ωcalc	ωscal	ωFT_IR	ωRaman	Assignment with PED* (%)
81	1014	974			ν (O7-C18)(20)+δ (H21-C4-C5)(17)+ν (O8-C18)(13)
82	1024	984	987w		ν (O3-C7)(21)+ν (O1-C7)(31)
83	1044	1003			ν (O7-C18)(12)
84	1049	1008			δ (H24-C12-N4)(13)+ν (C5-C4)(11)+δ (H9-O6-C2)(11)+δ (H18-O2-C9)(33)+ +δ (H22-C5-N2)(15)+δ (H9-O6-C2)(30)+δ (H18-O2-C9)(11)+ν (C11-C12)(10)
85	1058	1017			ν (O3-C7)(11)+τ (H6-C17-C15-C16)(15)+τ (H4-C16-C15-C17)(25)
86	1062	1021			ν (N1-C20)(13)+ν (O8-C18)(28)
87	1070	1028			τ (H14-C24-C22-C23)(17)+ν (O3-C7)(11)+ν (N3-C13)(19)+ +τ (H11-C23-C22-C24)(18)
88	1081	1039			ν (O7-C18)(13)
89	1087	1045	1041w		ν (O7-C18)(18)
90	1102	1059			δ (H1-C3-C4)(13)+ν (C3-C4)(10)+δ (H21-C4-C5)(11)
91	1104	1061			δ (H2-C10-C11)(13)+ν (C10-C11)(10)+δ (H23-C11-C12)(10)
92	1121	1077			δ (H24-C12-N4)(10)+ν (N4-C6)(15)+ν (N3-C6)(19)+δ (C12-N4-C6)(10)
93	1125	1081	1083vs		ν (N2-C1)(16)+δ (H22-C5-N2)(11)+δ (C1-N2-C5)(11)+ν (N1-C1)(21)
94	1216	1169	1143w		τ (H13-C23-C22-C24)(10)+τ (H15-C24-C22-C23)(19)
95	1221	1173			τ (H8-C17-C15-C16)(11)+τ (H3-C16-C15-C17)(14)
96	1233	1185	1186s		δ (H17-C7-O1)(20)+τ (H8-C17-C15-C16)(12)+ν (C16-C15)(12)
97	1237	1189			τ (H17-C7-O1-Zn1)(14)+δ (H17-C7-O1)(34)
98	1244	1195			ν (C23-C22)(14)+γ (C23-O8-O10-C22)(11)+τ (H16-C24-C22-C23)(12)
99	1268	1219	1213vs		ν (N4-C6)(26)+ν (N4-C12)(23)
100	1275	1225			ν (N2-C5)(17)+ν (N2-C1)(21)
101	1282	1232			τ (H17-C7-O1-Zn1)(26)
102	1295	1244		1239w	ν (O4-C14)(11)+τ (H17-C7-O1-Zn1)(13)
103	1298	1247			δ (H24-C12-N4)(10)+δ (H2-C10-C11)(19)+ν (N4-C12)(10)+ν (O2-C9)(21)
104	1299	1248			δ (H1-C3-C4)(15)+ν (O6-C2)(14)+ν (N2-C5)(10)
105	1307	1256	1257m		ν (O4-C14)(12)+ν (O10-C22)(16)
106	1323	1271	1270m		ν (O10-C21)(19)+ν (C21-C19)(17)
107	1334	1282	1294m	1282m	δ (H19-C20-C19)(65)
108	1360	1307	1305s	1305vw	δ (H20-C13-C8)(65)
109	1375	1321	1319m		τ (H10-C18-O7-Zn1)(38)
110	1388	1334	1351vs		ν (C9-C10)(14)+δ (H24-C12-N4)(12)+δ (H20-C13-C8)(10)+ν (N4-C6)(11)
111	1390	1336			τ (H10-C18-O7-Zn1)(19)
112	1423	1368	1371m	1351m	τ (H10-C18-O7-Zn1)(17)+δ (H10-C18-O7)(75)
113	1443	1387	1378s		ν (C10-C11)(14)+δ (C11-C12-N4)(14)+ν (O2-C9)(17)
114	1446	1390			δ (H3-C16-H5)(17)+δ (H4-C16-H3)(14)+δ (H5-C16-H4)(11)
115	1448	1392			ν (C3-C4)(13)+ν (O6-C2)(14)+δ (N2-C5-C4)(12)

Scientia Amazonia, v. 11, n.3, C16-C31, 2022
Revista on-line http://www.scientia-amazonia.org
https://doi.org/10.5281/zenodo.7510994 - ISSN:2238.1910

#	ωcalc	ωscal	ωFT_IR	ωRaman	Assignment with PED* (%)
116	1450	1393	1398m		δ (H15-C24-H14)(15)+δ (H12-C23-H11)(14)+δ (H11-C23-H13)(14)+ +δ (H16-C24-H15)(16)+δ (H14-C24-H16)(15)+δ (H13-C23-H12)(16)
117	1465	1408		1407vs	δ (H8-C17-H7)(31)+δ (H6-C17-H8)(16)+δ (H7-C17-H6)(16)+δ (H3-C16-H5)(20)
118	1468	1411			δ (H15-C24-H14)(12)+δ (H12-C23-H11)(10)+δ (H16-C24-H15)(23)+ +δ (H14-C24-H16)(10)+δ (H13-C23-H12)(30)
119	1504	1445	1432m		δ (H15-C24-H14)(13)+δ (H12-C23-H11)(14)+δ (H11-C23-H13)(41)
120	1506	1447			δ (H8-C17-H7)(11)+δ (H6-C17-H8)(18)+δ (H4-C16-H3)(33)+δ (H3-C16-H5)(15)
121	1508	1449			δ (H12-C23-H11)(13)+δ (H8-C17-H7)(18)+δ (H16-C24-H15)(31)+δ (H5-C16-H4)(19)+δ (H7-C17-H6)(34)+δ (H14-C24-H16)(19)+δ (H13-C23-H12)(13)
122	1525	1466	1456s	1468w	δ (H15-C24-H14)(16)+δ (H6-C17-H8)(18)+δ (H13-C23-H12)(15)+ +δ (H3-C16-H5)(14)+δ (H8-C17-H7)(12)
123	1533	1473			δ (H15-C24-H14)(19)+δ (H12-C23-H11)(19)+τ (H14-C24-C22-C23)(10)+ +δ (H14-C24-H16)(30)
124	1534	1474			δ (H6-C17-H8)(15)+δ (H7-C17-H6)(20)+δ (H5-C16-H4)(30)+δ (H4-C16-H3)(11)
125	1562	1501		1500vs	ν (C8-C13)(16)+ν (C9-C10)(23)+ν (C11-C12)(26)
126	1564	1503			ν (C19-C20)(10)+ν (C5-C4)(25)+δ (H1-C3-C4)(10)+ν (C2-C3)(29)
127	1585	1523			ν (C8-C13)(28)+ν (C11-C12)(18)
128	1588	1526			ν (C19-C20)(14)+δ (C2-C3-C4)(11)+ν (C3-C4)(12)+ν (C5-C4)(17)
129	1599	1537	1538vs		ν (C8-C13)(21)+ν (C9-C10)(15)+ν (C10-C11)(15)+δ (H2-C10-C11)(10)
130	1601	1539	1562m		ν (C19-C20)(37)+ν (C2-C3)(11)
131	1750	1682	1662s	1614m	ν (O5-C14)(86)
132	1754	1686			ν (O9-C21)(86)
133	2877	2765			ν (C7-H17)(98)
134	2908	2795			ν (C17-H7)(32)+ν (C24-H16)(29)+ν (C24-H14)(27)+ν (C17-H6)(28)+ +ν (C24-H15)(26)+ν (C17-H8)(29)
135	2916	2802			ν (C23-H12)(40)+ν (C23-H13)(25)+ν (C23-H11)(17)
136	2918	2804			ν (C16-H3)(31)+ν (C16-H5)(39)+ν (C16-H4)(18)
137	2973	2857			ν (C17-H7)(33)+ν (C16-H3)(18)+ν (C16-H5)(24)+ν (C17-H8)(17)
138	2974	2858			ν (C24-H16)(25)+ν (C23-H12)(30)+ν (C23-H13)(24)
139	2977	2861			ν (C24-H16)(13)+ν (C24-H15)(19)+ν (C24-H14)(60)
140	2978	2862			ν (C17-H7)(12)+ν (C17-H8)(17)+ν (C17-H6)(62)
141	2982	2866			ν (C16-H3)(11)+ν (C16-H4)(11)+ν (C16-H5)(26)+ν (C17-H8)(32)+ν (C17-H7)(18)
142	2983	2867			ν (C24-H16)(27)+ν (C23-H12)(17)+ν (C24-H15)(39)
143	2993	2876			ν (C16-H3)(32)+ν (C16-H4)(65)

Scientia Amazonia, v. 11, n.3, C16-C31, 2022
Revista on-line http://www.scientia-amazonia.org
https://doi.org/10.5281/zenodo.7510994 - ISSN:2238.1910
CIÊNCIA EXATAS E DA TERRA

#	ωcalc	ωscal	ωFT_IR	ωRaman	Assignment with PED* (%)
144	2997	2880			ν (C23-H13)(35)+ν (C23-H11)(63)
145	3037	2919	2948vw	2947vw	ν (C18-H10)(99)
146	3223	3097		3016vw	ν (C3-H1)(96)
147	3224	3098			ν (C10-H2)(96)
148	3269	3142	3120vw		ν (C20-H19)(100)
149	3293	3165			ν (C13-H20)(100)

* Only PED values greater than 10 % are given.
Caption: δ - in-plane bending, τ - torsion, γ - out-of-plane bending, ν - stretching.

All predicted vibrational modes are active in both Raman and infrared spectra. To a deeper study of $C_{24}H_{24}N_4O_{10}Zn$, we generated Figure 4, where we may observe experimental (above) and theoretical (below) Raman spectra and in Figure 5, we may also observe experimental (above) and theoretical (below) IR spectra. The theoretical spectra reported were scaled. We can observe from experimental spectrum, bands of medium intensity below 200 cm^{-1}, as shown in Figure 4, which are not observe in the calculated spectrum. This same region, beyond to some internal modes, we can find external ones that comprises lattice modes of the crystal. Since those modes are made in isolated molecules, they do not appear on the calculations. Therefore, there is a relevant probability that those modes contribute to the peaks in the Raman Spectrum of range. In the 1600 cm^{-1} region, some of the strongest Raman spectral peaks are expected.

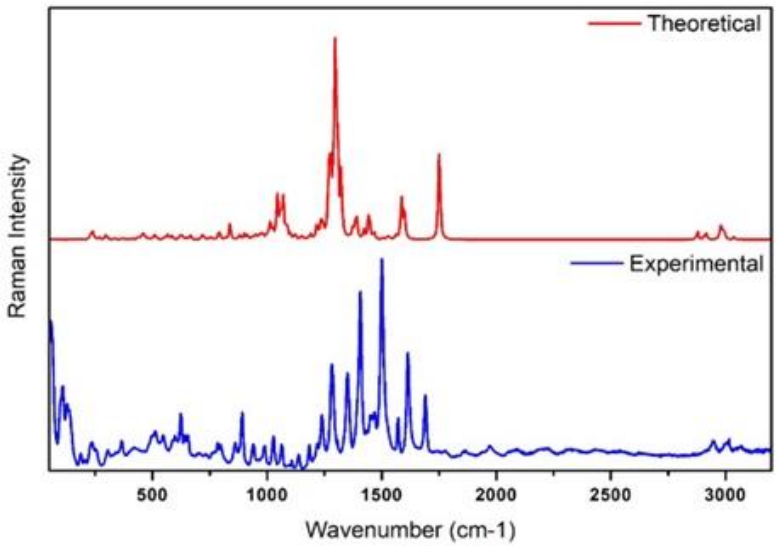

Figure 4: FT-Raman spectrum at ambient temperature of $C_{24}H_{24}N_4O_{10}Zn$ in the region 3250–50 cm^{-1}.

The correlation between empirical and calculated spectra is good. In particular, we note that the presence of the 1614 cm^{-1} band associated with O-C stretch vibration ν (O5-C14) belongs to the Meldrum's ring. We may note, also, that above 2900 cm^{-1}, observe bands relates to C–H stretching, ν (C-H), and O–H stretching, ν (O-H). Usually, while ν (O-H) bands have low intensities, on other hand, ν (C-H) bands have high intensities. The absence of this behavior on our spectra is due the kind of detector used, which is not very sensitive to

Scientia Amazonia, v. 11, n.3, C16-C31, 2022
Revista on-line http://www.scientia-amazonia.org
https://doi.org/10.5281/zenodo.7510994 - ISSN:2238.1910
CIÊNCIA EXATAS E DA TERRA

the spectral range above 3000 cm^{-1}. Now we shall discuss the experimental IR and Raman Spectrum in face of the theoretical one. The carbonyl stretching is a very intense peak observed in the range of 1600-1800 cm^{-1}. This special spectral region of infrared and Raman spectroscopy is important because it is sensitive to substitution effects and the geometry of the molecule, such as zinc complexation (KRISHNAKUMAR 2009).

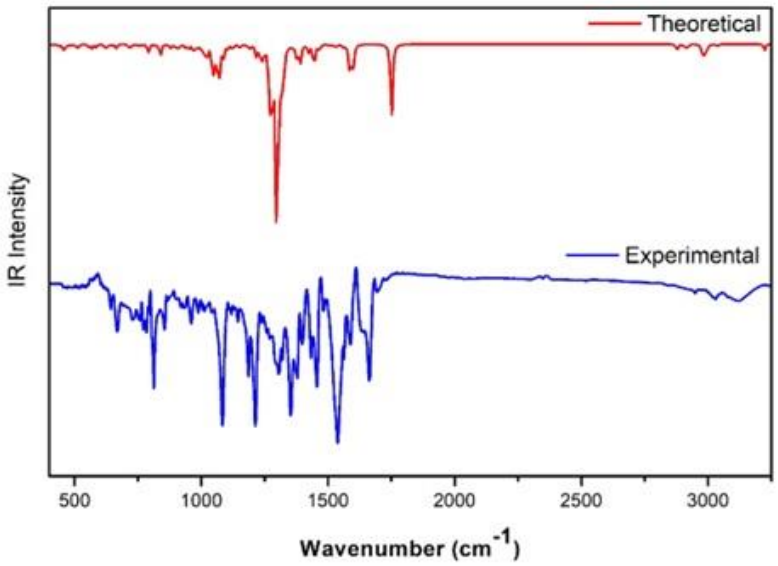

Figure 5: FT-IR spectrum at ambient temperature of $C_{24}H_{24}N_4O_{10}Zn$ in the region 3250–400 cm^{-1}.

The π conjugation is observed and it is predicted in vibrational spectra for carbonyl mode. The carbonyl stretching is observed for $C_{24}H_{24}N_4O_{10}Zn$ at 1662 cm^{-1} in FT Raman and at 1614 cm^{-1} FT-IR spectra with PED contribution of 86%. This mode was predicted at 1750 cm^{-1} by DFT calculations. We can also find several C-O stretches in the fingerprint region (between 1200 and 1000 cm^{-1}) in the predicted Raman spectra with PED contributions no higher than 32%, those single bonded C-O are compatible with our compound since it is an acid derivative (MAYO 2004). The aromatic C-C stretching modes are expected to be found between 1650 and 1200 cm^{-1} (SUBRAMANIAN 2011; WEAST 1977). The C(8)-C(13) stretching vibrations were observed at 1538 cm^{-1} in FT-IR spectrum and at 1500 cm^{-1} in FT-Raman, this is due very strong stretches occurring inside Pyridine ring **B1**, so it is expected to find similar behavior at C(9)-C(10) and C(10)-C(11), since six-membered heterocyclics systems behave in similar fashion to benzene analog, we can also observe that the strong stretch that occurs at 1378 cm^{-1} at FT-IT spectra is also due this mimic of a monosubstituted phenyl system by the pyridine (MAYO 2004). We can find the C-H deformation (bending) vibrations modes of the methyl group at 1456, 1432 and 1398 cm^{-1} in FT-IR and at 1468 and 1407 cm^{-1} in FT-Raman, related to with methyl radicals from both Meldrum's acid rings, A and A1.

The umbrella modes (single symmetric deformations) are 1398 cm^{-1} for the first and 1407 cm^{-1} for the latter (MAYO 2004). Between 1350 and 1000 cm^{-1} we can find a mix of types of vibration. Single C-O vibrational stretching modes are expected to appear in this fingerprint region, usually more visible at FR-IR, we found it at 1270 and 1257 cm^{-1}. Also, it

Scientia Amazonia, v. 11, n.3, C16-C31, 2022
Revista on-line http://www.scientia-amazonia.org
https://doi.org/10.5281/zenodo.7510994 - ISSN:2238.1910

was expected to find the very unique vibrational modes in this region, in our case, the ones involving the Zinc: they are torsions with H(10)-C(18)-O(7)-Zn(1) occurring at 1371 and 1319 cm^{-1} in FT-IR spectrum, with PED contribution of 17% and 38% respectively, and 1351 cm^{-1} FT-Raman with 37% of contribution. Vibrational stretching of N-C single bonds were found at 1213 cm^{-1} and HCO bending at 1186 cm^{-1} in FT-IR spectrum. The torsional modes assigned to HCCC were supposed to be found between 1200 and 890 cm^{-1} and indeed were found at 891 at experimental FT-Raman and at 1186, 1143, 917 and 854 FT-IR spectrum, as expected. Note that, in the latter, there is a Pyridine ring **B1** puckering mode. We also can find vibrational stretching modes assigned to simple bonds of C-O at 1000 cm^{-1} region, in the experimental FT-IR we registered at 1041 and 987 cm^{-1} but were not observed in the FT-Raman spectrum. Those modes were involved on the complexation process and reinforces that the oxygen took part on it. The computed wavenumber by B3LYP/6-31G (d, p) method in the range 766-620 cm^{-1} are assigned to aromatic out-of-plane bending of OCCC and CCOC. They were observed in FT-Raman spectrum at 623 cm^{-1} and at 771, 757, 667 and 642 cm^{-1} in FT-IR spectrum. It is relevant note that there is a Meldrum's ring **A** puckering mode at 667 cm^{-1}, according to FT-IR. The wavenumbers predicted at 495 and 132 cm^{-1}, correspond to the FT-Raman bands observed at 499 and 127 cm^{-1}, respectively, and are associated to HCCN torsion and CCC in-plane bending. Finally, we registered weak peak of a vibrational stretching of Zn-N at 108 cm^{-1} of experimental FT-Raman, that may refer to the complexation process. This mode was expected to appear at 190 cm^{-1} (BENAVIDES 2007).

3.3 Thermodynamics

The various statistical thermodynamic parameters viz. thermal energy, entropy, specific heat, and zero-point vibrational energy (ZPVE) of the target complex were computed at T = 298.15K and the corresponding values were listed in Table 3.

Table 3 - Some standard thermodynamical parameters.

Parameters	$C_{24}H_{24}N_4O_{10}Zn$
Thermal energy (kcal/mol)	312.053
Specific heat (C_V) (cal/mol-k)	127.717
Entropy (S) (cal/mol-k)	194.837
ZPVE (kcal/mol)	292.49155

Besides, the contribution of total (Electronic + Rotational + Translational + Vibrational) motions in magnitude of these parameters, we have also considered vibrational contribution. The table infers that the magnitude of thermal energy and specific heat is mainly due to the vibrational motion whereas the contribution of vibrational motion is nearly 64% in case of entropy. Hence, the contribution of rest three motions (Electronic + Rotational + Translational) appears by 36% in entropy. Moreover, the zero-point vibrational energy was calculated to be 292.49155 Kcal/mol.

4. Conclusions

In the present paper, a spectroscopy analysis using FT-Raman and FTIR techniques combined with DFT/B3LYP/6-31G (d,p) basis set theoretical calculations allowed the investigation of the structural and vibrational properties of the Meldrum's acid derivative $C_{24}H_{24}N_4O_{10}Zn$. The geometry parameters and the vibrational wavenumbers of the

molecule were calculated, and the optimized structures was found to be a non-planar structure. Furthermore, theoretical results indicate that π conjugation tends to be in the region close to carbonyl. The calculated (scaled) vibrational spectra was compared and assigned with FT-IR and FT-Raman, assisted by quantum chemical theoretical calculations, that was used to characterize the $C_{24}H_{24}N_4O_{10}Zn$. Finally, this study has contributed with a description of vibrational spectra and geometrical parameters analysis of a compound with potential antiviral activity.

Acknowledgement

The authors would like acknowledgement the financial support from FAPEMAT, CNPq and FUNCAP. We thank Professor R. G. Freitas for computational facilities made available through the project "proj650" register on CENAPAD-SP for the use of the Gaussian 09 software package.

Disclosure

This article is unpublished and is not being considered for any other publication. The author(s) and reviewers did not report any conflict of interest during their evaluation. Thus, the journal Scientia Amazonia holds the copyright, has the approval and permission of the authors to disclose this Article electronically.

References

A.S. Ivanov. Chem. Soc. Rev. 37 (2008) 789-811.

A.N. Meldrum. J. Chem. Soc. 93 (1908) 598.

A. Chaudhary, P. Saluja and J. M. Khurana, Current Green Chemistry 3 (2016) 328.

A. D. Becke, Physical Review A, 38 (1988) 3098-3100.

A. Tapia-Benavides, M. Tlahuextl, H. Tlahuext, C. Galán-Vidal, Arkivoc, 2008 (2007) 172-186.

B. Schrader, B. Dippel, I. Erb. J. Mol. Struct. 481 (1999) 21–32.

B. Schrader, H.H. Klump, K. Shenzel. J. Mol. Struct. 509 (1999) 201–212.

B. C. Chen. Heterocycles. 32 (1991) 529-597.

C. Mayo, T. Teslova, M. V. Cañamares, Z. Chen, J. Zhang, J. R. Lombardi, M. Leona, Vibrational Spectroscopy. 49 (2009) 190-195.

C. Lee, W. Yang, R. G. Parr, Physical Review B, 37 (1988) 785-789.

D.V. Sevenard, A.V. Didenko, D. Lorenz, M. Vorobiev, J. Stelten, T. Dulcks, V. Ya. Sosnovskikh. Tetrahedron 73 (2017) 1495-1502.

D.W. Mayo, F.A. Miller and R.W. Hannah, Course Notes on the Interpretation of Infrared and Raman Spectra, John Wiley & Sons, Inc., Hoboken, 2004.

E. Urlaub, J. Popp, W. Kiefer. Biospectroscopy 4 (1997) 113 -120.

G.M.M. Sampaio, A.M.R. Teixeira, H.D.M. Coutinho, D.M. de Sena Junior, P.T.C. Freire, P.E.S. Caselli, G.O.M. Gusmão, R.R.F. Bento, L.E. Silva. J. Mol. Struct. 1038 (2013) 170-176.

G.M.M. Sampaio, A.M.R. Teixeira, H.D.M. Coutinho, D.M. de Sena Junior, P.T.C. Freire, R.R.F. Bento, L.E. Silva, EXCLI Journal, 13 (2014) 1022-1028.

G. Genova, S. Della Chiesa, T. Mimmo, L. Borruso, S. Cesco, E. Tasser, A. Matteazzi, G. Niedrist, Copper and zinc as a window to past agricultural land-use, Journal of Hazardous Materials, Volume 424, Part C (2022).

H. McNab. Chem. Soc. Rew. 7 (1987) 345.

H.F. Mohssen, N.M. Ali, H.A. Ali, J. Chem. Pharm. Res. 9 (2017) 209-219.

I. Yavari. Journal of Physical & Theoretical Chemistry. 2(3) (2005) 3-8.

J. P. Abraham, D. Sajan, J. Mathew, I. Hubert Joe, V. George, V. S. Jayakumar, Journal of Raman Spectroscopy. 39 (2008) 1821-1831.

Joule, J. A.; Mills, K. Heterocyclic Chemistry (5th ed.). Chichester: Blackwell Publishing (2010).

J-Y. Shi, J-Q. Li, R-S. Tong, H. Lin, C. Lu. Acta crystallographica. Section E, Structure reports online. 67 (2011) 253.

K. Janikowska, J.Rachon, S. Makowiec. Russian Chemical Reviews 83 (2014) 620-637.

K. Radotic, M. Micic, M. Jeremic, Annals New York Acad. Sci. 1048 (2005) 215– 229.

K. Janikowska, J. Rachoń, S. Makowiec. Russian Chemical Reviews. 83(7) (2014) 620–637.

L.E. Silva, A.C. Joussef, L.K. Pacheco, D.B.L. Albino, A.M.C. Duarte, M. Steindel, R.A. Rebelo, Letters in Drug Design & Discovery. 4 (2007) 154-159.

M. Micic, K. Radotic, M. Jeremic, Macromol. Biosc. 3 (2003) 100–106.

[17-28] M. Fehr, D.W. Ehrhardt, S. Lalonde, Cur. Opin. Plant Biol. 7 (2004) 345–351.

M. Daci-Ajvazi, S. Govori, S. Omeragiq. E-Journal of Chemistry. 8(4) (2011) 1522–1527.

M. H. Jamróz, J. C. Dobrowolski, J. Mol. Struct., 565-566 (2001) 475-480.

N. Subramanian, N. Sundaraganesan, S. Sudha, V. Aroulmoji, G. D. Sockalingam, M. Bergamin, Spectrochim. Acta, Part A, 78 (2011) 1058-1067.

National Center for Biotechnology Information (NCBI) (2022). PubChem Compound Summary for CID 2819737. Retrieved February 12, 2022 from https://pubchem.ncbi.nlm.nih.gov/compound/2819737.

[29-33] N. Subramanian, N. Sundaraganesan, J. Jayabharathi, Spectrochim. Acta, Part A, 76 (2010) 259-269.

P. Sinha, S.E. Boesch, C. Gu, R.A. Wheeler, A.K. Wilson, The Journal of Physical Chemistry A, 108 (2004) 9213-9217.

R. Weast, D. R. Lide, Cleveland, Ohio: CRC Press, 1977.

R. Çaliskan, N. Nohut, O. Yilmaz, E. Sahin, M. Balci. Tetrahedron 73 (2017) 291-297.

S. Ghosh, J. Das, S. Chattopadhyay. Tetrahedron Letters 52 (2011) 2869-2872.

S.M. Shahcheragh, A. Habibi, S. Khosravi. Tetrahedron Letters 58 (2017) 855-859.

S. V. Lindeman, Yu. T. Struchkov, O. V. Shishkin, S. M. Desenko, V. V. Lipson, V. D. Orlov. Acta Cryst. 49 (1993) 896-898.

T. A. de Toledo, L.E. da Silva, T.C. Botelho, R.J. Ramos, P.T. Souza Jr., A.M.R. Teixeira, P.T.C. Freire, R.R.F. Bento. Journal of Molecular Structure. 1029 (2012) 22-27.

V.V. Lipson, N.Yu. Gorobets. Mol Divers. 13 (2009) 399-419.

V. Krishnakumar, M. Sivasubramanian, S. Muthunatesan, J. Raman Spectrosc. 40 (2009) 987-991.

W. Kohn, A. D. Becke, R. G. Parr, The Journal of Physical Chemistry, 100 (1996) 12974-12980.

Scientia Amazonia, **v. 11, n.3, C16-C31, 2022**
Revista on-line http://www.scientia-amazonia.org
https://doi.org/10.5281/zenodo.7510994 - ISSN:2238.1910

Y. Yoshikawa, H. Yasui, Current Topics in Medicinal Chemistry 12 (2012) 210.

Z. Dhaouadi, M. Nsangou, N. Garrab, E. H. Anouar, K. Marakchi, S. Lahmar, J. Mol. Struct. 904 (2009) 35-42.